The RFI 2022 Workshop at ECMWF, 14 – 18 February 2022
2022 URSI International Union of Radio Science

Polarization Sensitive Array Reconfiguration Method Based on Antenna Selection for GNSS Interference Suppression

Yandong Sun(1), Jian Xie*(1), Chuang Han(1), and Ling Wang(1)
(1) School of Electronics and Information, Northwestern Polytechnical University, Xi'an 710072, China

Abstract

Polarization-sensitive array (PSA) has been widely used in global navigation satellite system (GNSS) applications for interference rejection. However, traditional PSA configuration where each antenna fixedly connects with two or more radio frequency (RF) front ends can result in large computational complexity and even redundancy in performance. To achieve a high signal to interference plus noise ratio (SINR) with fewer antennas and RF front ends, A PSA reconfiguration strategy based on antenna selection was proposed in this paper. The polarization-spatial correlation coefficient (PSCC) is proposed to describe the degree of separation between desired signal and interference in the polarization-spatial domain. We derive the relational expression of SINR and PSCC, and analyze the impact of array reconfiguration on PSA performance. Aiming at maximizing the SINR of reconstructed PSA, we calculate the upper bounds of SINR and plot the curve between computational cost and SINR loss to guide the selection of antenna quantity. And we present two approaches to solve the selection problem more efficiently, instead of by enumeration. The experiment results validate that even utilizing a handful of antennas and RF front ends, it is still possible to yield high SINR by PSA reconfiguration. And the proposed reconfiguration approaches are quite effective in improving efficiency as well as achieving superior interference suppression performance.

1 Introduction

Polarization-sensitive array (PSA) has extensive application prospect in global navigation satellite system (GNSS) due to its potential to enhance interference suppression performance [1–3]. Compared with the scalar array, the PSA works better in anti-interference as it can filter the interference in the polarization-spatial domain. Nevertheless, the conventional PSA architecture where each polarized antenna has to be connected to multiple radio frequency (RF) front ends causes great redundancy in software and hardware costs [4]. On the one hand, more and more antennas and RF front ends are utilized to acquire better performance in the array system, leading to a sharp increase in hardware overhead. On the other hand, using multiple antennas also increases the computational complexity of adaptive processing. Therefore, it becomes a topic worthy of study to use fewer antennas to obtain high interference suppression performance.

The array configuration was first considered as an available degree of freedom (DOF) in [5] to improve the anti-interference performance, implemented by using some RF switches. Resorting to the RF switch, the on-off state between antenna and RF front end can be controlled, and a part of antennas are appointed to constitute the reconstructed array. Inspired by the above method, Several array reconfiguration approaches were proposed to gain the thinning array, such as heuristic method [6], Matrix Pencil method [7], and Bayesian inference algorithm [8]. However, these methods are a little inefficient owing to high computational complexity or poor convergence. To precisely measure the effect of array reconfiguration on anti-jamming performance, a parameter, called spatial correlation coefficient (SCC), was proposed [9, 10]. After that, a few reconfiguration methods were presented to apply to beamforming [11, 12]. In recent years, the research on array reconfiguration has been extended to multiple-input multiple-output (MIMO) and other fields [13, 14].

Although much research has been done on scalar array reconfiguration, there is little work regarding PSA reconfiguration. And the reconfiguration approaches mentioned above cannot be used directly for PSA. In this paper, we propose a new technique based on antenna selection to guide the PSA reconfiguration. With analysis of the optimal signal to interference plus noise ratio (SINR) of PSA, we explore the array configuration factors affecting performance and present the polarization-spatial correlation coefficient (PSCC). Then two approaches are developed to gain the optimal PSA, which employs the fewest antennas to obtain the maximum SINR. And the RF switch is adopted to complete the PSA reconfiguration.

2 Signal Model and Problem Formulation

In this section, we present the signal model and formulate the objective function of PSA reconfiguration.

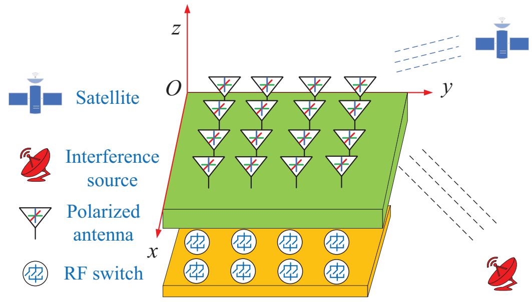

Figure 1. Reconfigurable PSA comprising N tri-orthogonal electric dipole antennas. And M antennas are selected (e.g., $N = 16, M = 8$).

2.1 Signal Model

Consider a PSA comprising N tri-orthogonal electric dipole antennas, as shown in Fig. 1. All the tri-orthogonal electric dipoles, uniformly placed on the $x-y$ plane with an interval of d, consist of three orthogonal dipoles with coincident spatial phase centers. And three orthogonal dipoles point in the directions of the x-axis, y-axis, and z-axis, respectively. Each antenna corresponds to three RF switches that can control the on-off state between the antenna and RF front end. Resorting to the RF switches, we can choose a part of antennas to constitute a new PSA.

Assume that the desired signal is incident on the PSA from (θ_s, ϕ_s), where θ and ϕ severally denote the elevation and azimuth of the desired signal. Correspondingly, the interference is coming from (θ_i, ϕ_i) in single interference scenario. And the two-dimension direction of arrival (DOA) vectors of the desired signal and interference can be formulated as

$$\begin{aligned}\mathbf{v}_j &= \begin{bmatrix} v_{xj} & v_{yj} & v_{zj} \end{bmatrix}^T \\ &= \left[\sin\theta_j \cos\phi_j \quad \sin\theta_j \sin\phi_j \quad \cos\theta_j\right]^T, j = s, i,\end{aligned} \quad (1)$$

where $(\cdot)^T$ represents the transpose of a matrix. Then the spatial steering vectors of desired signal and interference can be written as

$$\mathbf{a}_j = e^{j\frac{2\pi}{\lambda}\mathbf{P}\mathbf{v}_j} = e^{jk_0\mathbf{P}\mathbf{v}_j}, j = s, i, \quad (2)$$

where $\mathbf{P}$ is the coordinate matrix of N antennas and λ denotes the wavelength of desired signal.

$$\begin{aligned}\mathbf{P} &= \left[\mathbf{p}_1^T, \mathbf{p}_2^T, \dots, \mathbf{p}_N^T\right]^T \\ &= \begin{bmatrix} x_1 & y_1 & z_1 \\ x_2 & y_2 & z_2 \\ \vdots & \vdots & \vdots \\ x_N & y_N & z_N \end{bmatrix}.\end{aligned} \quad (3)$$

And $\mathbf{p}_n = [x_n, y_n, z_n]$ for $n = 1, 2, \cdots N$ denotes the position coordinate vector of the n_{th} antenna.

Under the case that the sensed signals are completely polarized, the polarization characteristics of the desired signal and interference can be described by the amplitude-phase descriptors (γ_s, η_s) and (γ_i, η_i). And γ and η are the polarization auxiliary angle and polarization phase difference, respectively, and $0 \le \gamma \le \pi/2$, $-\pi < \eta \le \pi$. Particularly, the received satellite signal in GNSS is right-handed circular polarized (RHCP), and $\gamma_s = 0.25\pi$ and $\eta_s = -0.5\pi$. Hence, the polarization steering vectors of the desired signal and interference can be obtained as

$$\begin{aligned}\mathbf{u}_{pj} &= \begin{bmatrix} E_{xj} \\ E_{yj} \\ E_{zj} \end{bmatrix} \qquad j = s, i \\ &= \begin{bmatrix} -\sin\phi_j & \cos\theta_j\cos\phi_j \\ \cos\phi_j & \cos\theta_j\sin\phi_j \\ 0 & -\sin\theta_j \end{bmatrix} \begin{bmatrix} \cos\gamma_j \\ \sin\gamma_j e^{j\eta_j} \end{bmatrix}.\end{aligned} \quad (4)$$

According to (2) and (4), the polarization-spatial domain joint steering vectors of desired signal and interference are expressed as

$$\mathbf{s}_{pj} = \mathbf{a}_j \otimes \mathbf{u}_{pj} \in \mathbb{C}^{3N\times 1}, j = s, i, \quad (5)$$

with $\otimes$ representing the Kronecker product.

Then the signals received by PSA can be given by

$$\begin{aligned}\mathbf{X}(t) &= \mathbf{s}_{ps}s_s(t) + \mathbf{s}_{pi}s_i(t) + \mathbf{n}(t) \\ &= \mathbf{s}_{ps}s_s(t) + \mathbf{X}_{i+n}(t),\end{aligned} \quad (6)$$

where $s_s(t)$ and $s_i(t)$ are the complex envelopes of desired signal and interference, respectively, and $\mathbf{n}(t)$ denotes the white noise.

2.2 Problem Formulation

Based on (6), we assume that the interference and noise are independent of each other, then the interference plus noise covariance matrix can be acquired as follows:

$$\begin{aligned}\mathbf{R}_n &= E\left\{\mathbf{X}_{i+n}(t)\left(\mathbf{X}_{i+n}(t)\right)^H\right\} \\ &= \sigma_n^2\mathbf{I}_{3N} + \sigma_i^2\mathbf{s}_{pi}\mathbf{s}_{pi}^H\end{aligned} \quad . \quad (7)$$

with σ_n^2 and σ_i^2 severally representing the power of noise and interference. And $\mathbf{I}_{3N}$ is a $3N \times 3N$ unit matrix and $(\cdot)^H$ means the conjugate transpose of a matrix. Note that $\mathbf{s}_{pi}^H\mathbf{s}_{pi} = \mathbf{s}_{ps}^H\mathbf{s}_{ps} = N$, the inverse covariance matrix can be formulated as

$$\mathbf{R}_n^{-1} = \sigma_n^{-2}\left(\mathbf{I}_N - \frac{\mathbf{s}_{pi}\mathbf{s}_{pi}^H}{\frac{\sigma_n^2}{\sigma_j^2} + N}\right). \quad (8)$$

Resorting to the Minimum Variance Distortionless Response (MVDR) algorithm [15], the optimal weight vector of adaptive processing can be expressed as

$$\begin{aligned}\mathbf{W}_{\text{opt}} &= \xi\mathbf{R}_n^{-1}\mathbf{s}_{ps} \\ &= \frac{\xi}{\sigma_n^2}\left(\mathbf{s}_{ps} - \frac{\mathbf{s}_{pi}\mathbf{s}_{pi}^H\mathbf{s}_{ps}\cdot \text{INR}}{1 + N\cdot \text{INR}}\right),\end{aligned} \quad (9)$$

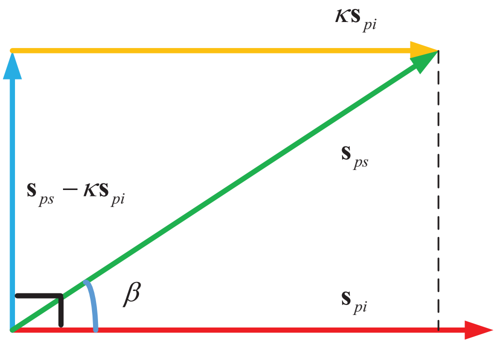

Figure 2. The relationship between PSCC and two polarization-spatial domain joint steering vectors.

where $\mathrm{INR} = \sigma_i^2/\sigma_n^2$ denotes interference to noise ratio and ξ is an ignorable constant that cannot affect the performance. Accordingly, the optimal output SINR is obtained as

$$\begin{aligned} \mathrm{SINR}_{\mathrm{out}} &= \sigma_s^2 \mathbf{s}_{ps}^H \mathbf{W}_{\mathrm{opt}} \\ &= \mathrm{SNR}\left(N - \frac{\mathbf{s}_{ps}^H \mathbf{s}_{pi} \mathbf{s}_{pi}^H \mathbf{s}_{ps} \cdot \mathrm{INR}}{1 + N \cdot \mathrm{INR}}\right). \end{aligned} \tag{10}$$

where $\mathrm{SNR} = \sigma_s^2/\sigma_n^2$ means signal to noise ratio with σ_s^2 being the power of the desired signal.

Here, we define the PSCC between the desired signal and interference as

$$\kappa = \frac{\mathbf{s}_{pi}^H \mathbf{s}_{ps}}{\|\mathbf{s}_{pi}\| \cdot \|\mathbf{s}_{ps}\|} = \frac{\mathbf{s}_{pi}^H \mathbf{s}_{ps}}{\sqrt{\mathbf{s}_{pi}^H \mathbf{s}_{pi}} \sqrt{\mathbf{s}_{ps}^H \mathbf{s}_{ps}}} = \frac{\mathbf{s}_{pi}^H \mathbf{s}_{ps}}{N}, \tag{11}$$

where $\|\cdot\|$ denotes the Euclidean norm. Then, the relationship between PSCC and two polarization-spatial domain joint steering vectors can be illustrated in Fig. 2. And we can learn that the value of PSCC can be taken as the cosine of the angle between the desired signal and interference steering vectors in the polarization-spatial domain, and $|\kappa| \le 1$. Besides, the higher the $|\kappa|$ is, the closer the desired signal is to interference in the polarization-spatial domain, the more difficult the signal is to separate from the interference. In particular, the PSCC becomes 0 when the desired signal is orthogonal to the interference, which is the most expected in adaptive processing. Thus, the PSCC can describe the difference between the desired signal and interference in the polarization-spatial domain, and minimizing $|\kappa|$ contributes to the improvement of anti-interference performance.

Substituting (11) into (10), we convert the expression of the optimal SINR into the following form:

$$\mathrm{SINR}_{\mathrm{out}} = N \cdot \mathrm{SNR}\left(1 - |\kappa|^2 \frac{N \cdot \mathrm{INR}}{1 + N \cdot \mathrm{INR}}\right) . \tag{12}$$

Set χ as

$$\chi = \frac{N \cdot \mathrm{INR}}{1 + N \cdot \mathrm{INR}}. \tag{13}$$

Since we focus on the case that the interference power is much stronger than the noise power, χ is approximately equal to 1. Then (12) becomes

$$\mathrm{SINR}_{\mathrm{out}} = N \cdot \mathrm{SNR}\left(1 - |\kappa|^2\right) . \tag{14}$$

According to (14), we know that the interference suppression performance is affected by antennas number and the PSCC. And the anti-interference performance can be enhanced by altering the PSA configuration to generate a smaller PSCC when the quantity of antennas is confirmed. Therefore, the problem of maximizing SINR can be transformed into the minimizing PSCC problem, i.e.,

$$\max\left\{\mathrm{SINR}_{\mathrm{out}}\right\} \Rightarrow \min\left\{|\kappa|^2\right\}. \tag{15}$$

In the following, we devote ourselves to seeking the optimal array configuration that can minimize the PSCC.

3 PSA Reconfiguration Approaches

In this section, we convert the PSA reconfiguration problem based on antenna selection to a specific mathematical model and give two effective reconfiguration approaches. And the following processing operates on the condition that the DOA and polarization parameters belong to prior information.

With the purpose of selecting M antennas out of N to reconstruct the PSA enjoying the smallest PSCC ($M < N$), we define $\mathbf{z} \in \mathbb{R}^{N \times 1}$ as the antenna selection vector. $\mathbf{z}$ is only composed of zeros and ones, i.e., $z_j = 0$ or 1 for $j = 1, 2, \ldots, N$, and 0 indicates that the corresponding antenna is not selected, and 1 denotes the selected one. Combining (5) and (11), we formulate the expression of PSCC under antenna selection as

$$|\kappa| = \frac{\left|\mathbf{z}^T \mathbf{a}_{is}\right|}{M} \cdot \left|\mathbf{u}_{pi}^H \mathbf{u}_{ps}\right| \Leftrightarrow |\kappa|^2 = \frac{\mathbf{z}^T \mathbf{V}_r \mathbf{z}}{M^2} \cdot \left|\mathbf{u}_{pi}^H \mathbf{u}_{ps}\right|^2, \tag{16}$$

where $\mathbf{a}_{is} = e^{jk_0 \mathbf{P}(\mathbf{v}_s - \mathbf{v}_i)}$ denotes the spatial correlation vector of the desired signal and interference, and $\mathbf{V}_r = \mathrm{real}\left(\mathbf{a}_{is}\mathbf{a}_{is}^H\right)$ with $\mathrm{real}(\cdot)$ meaning the real part. Then, according to (15), the mathematical model of the antenna selection problem can be established as below.

$$\begin{aligned} \min_{\mathbf{z}} \quad & \left\{|\kappa|^2 = \frac{\mathbf{z}^T \mathbf{V}_r \mathbf{z}}{M^2} \cdot \left|\mathbf{u}_{pi}^H \mathbf{u}_{ps}\right|^2\right\} \\ \text{s.t.} \quad & z_j(z_j - 1) = 0 \quad j = 1, 2, \ldots, N \\ & \mathbf{z}^T \mathbf{z} = M. \end{aligned} \tag{17}$$

And the two constraint conditions separately indicate that the elements of $\mathbf{z}$ are binary, and M antennas are chosen. Note that the binary constraint leads to the non-convexity of the problem, and it is impossible to address it directly with convex optimization methods. Therefore, we develop two approaches to handle the above problem effectively.

3.1 SDP Approach

To solve the lower bound of the optimal PSCC in (17), we adopt a relaxation method, called the direct semidefinite programming (SDP). Firstly, we define a new optimization variable $\mathbf{Z} \in \mathbb{R}^{N\times N}$. Then the antenna selection problem in (17) can be reformulated as

$$\begin{aligned} \min_{\mathbf{Z}} & \frac{\left|\mathbf{u}_{pi}^H \mathbf{u}_{ps}\right|^2}{M^2} \operatorname{tr}(\mathbf{Z}\mathbf{V}_r) \\ \text{s.t. } & \mathbf{Z} = \mathbf{z}\mathbf{z}^T \\ & \operatorname{diag}(\mathbf{Z}) = \mathbf{z} \\ & \operatorname{tr}(\mathbf{Z}) = M, \end{aligned} \quad (18)$$

where $\operatorname{diag}(\cdot)$ denotes the vectorization of diagonal elements of matrix, and $\operatorname{tr}(\cdot)$ represents the trace of a matrix. The binary constraint in (17) is guaranteed by $\mathbf{Z} = \mathbf{z}\mathbf{z}^T$ and $\operatorname{diag}(\mathbf{Z}) = \mathbf{z}$. And the constraint $\operatorname{tr}(\mathbf{Z}) = M$ make it available to select M antennas. However, the existence of $\mathbf{Z} = \mathbf{z}\mathbf{z}^T$ causes the problem to remain nonconvex. Thus, we relax it to $\mathbf{Z} \succeq \mathbf{z}\mathbf{z}^T$ where $\succeq$ indicates that the matrix is semidefinite. Based on the matrix Schur complement lemma, the optimization problem of (18) is transformed into

$$\begin{aligned} \min_{\mathbf{Z}} & \frac{\left|\mathbf{u}_{pi}^H \mathbf{u}_{ps}\right|^2}{M^2} \operatorname{tr}(\mathbf{Z}\mathbf{V}_r) \\ \text{s.t. } & \begin{bmatrix} \mathbf{Z} & \mathbf{z} \\ \mathbf{z}^T & 1 \end{bmatrix} \succeq 0 \\ & \operatorname{diag}(\mathbf{Z}) = \mathbf{z} \\ & \operatorname{tr}(\mathbf{Z}) = M. \end{aligned} \quad (19)$$

The problem in (19) belongs to a semidefinite programming problem (SDP) [16] with two variables $\mathbf{Z}$ and $\mathbf{z}$. And we can employ a package for solving the convex problem, referred to as CVX [17, 18], to solve the optimal solution. It can be demonstrated that the optimal solution $|\kappa_{\text{opt}}|^2$ acquired with semidefinite convex optimization is a lower bound of the optimal PSCC, i.e.,

$$|\kappa_{\text{opt}}|^2 \leq |\kappa|^2. \quad (20)$$

Substituting (20) into (14), we formulate the upper bound of the optimal SINR as

$$\text{SINR}_{\text{out}} \leq M \cdot \text{SNR}\left(1 - |\kappa_{\text{opt}}|^2\right) \quad . \quad (21)$$

We can learn that the performance of all PSAs comprising M antennas cannot exceed the upper bound solved in (21). Besides, the number of antennas also influences the expenditures on hardware and software. Hence, (21) also reveals the tradeoff between anti-jamming performance and cost. And we show the process of choosing the optimal number of antennas as follows.

Firstly, taking the performance and computational cost of the primal PSA as a reference, we define two parameters $\text{SINR}_{\text{loss}}$ and O_{cost}, called normalized performance loss and normalized computational cost, respectively.

$$\text{SINR}_{\text{loss}}(M) = \text{SINR}_{\text{re}}(M) - \text{SINR}_{\text{pr}} \ \ (\text{dB}) \quad (22)$$

$$O_{\text{cost}}(M) = \frac{O_{\text{re}}(M)}{O_{\text{pr}}} = \frac{M^3}{N^3}, M = 2, \ldots, N \quad (23)$$

SINR_{pr} and SINR_{re}, calculated with (21), separately denote SINR of PSA before and after reconfiguration. Here, since the computational complexity of adaptive processing mainly focuses on matrix inversion, which possesses order $(M)^3$ complex operations for a $M \times M$ matrix, we utilize the computational cost of matrix inversion to substitute the cost of the whole processing. And O_{pr} and O_{re} severally represent the computational cost of PSA before and after reconfiguration. The normalized performance loss and computational cost characterize the effect of antennas number on PSA reconfiguration. According to (22) and (23), considering the O_{cost} and $\text{SINR}_{\text{loss}}$ as x-axis and y-axis, respectively, we obtain the trade-off curve between the computational cost and performance loss for different numbers of antennas. To still maintain high SINR after PSA reconfiguration, we set the constraint that the normalized performance loss cannot exceed ε dB, i.e., $|\text{SINR}_{\text{loss}}| \leq \varepsilon$ dB. Subsequently, through analyzing the trade-off curve, we select the M that can meet the above constraint and save the most cost as the optimal number of antennas for PSA reconfiguration.

3.2 CM Approach

Although it is effective to use the SDP approach to solve the upper bound of the optimal SINR to guide the selection of the optimal number of antennas, there is no way to acquire the positions of antennas directly due to the relaxation operation. Hence, we use a greedy search method, named correlation measurement (CM) to obtain the layout of the reconstructed PSA.

According to (16), the PSCC can be transformed into the following form:

$$|\kappa|^2 = \mathbf{z}^T \hat{\mathbf{V}} \mathbf{z} = \sum_{m,n=1}^{N} \mathbf{z}(m)\mathbf{z}(n)\hat{\mathbf{V}}_{mn} \quad (24)$$

with $\hat{\mathbf{V}} = \frac{\left|\mathbf{u}_{pi}^H \mathbf{u}_{ps}\right|^2}{M^2} \mathbf{V}_r$. It can be seen that the $|\kappa|^2$ is the sum of all chosen entries in $\hat{\mathbf{V}}$. Unde the case that the optimal number of antennas M has been confirmed, we calculate the sum of each row of the matrix $\hat{\mathbf{V}}$ and obtain the largest one by comparison during each iteration, e.g., the i_{th} row, which means that the i_{th} antenna possesses the maximum correlation measurement with all remaining antennas. Then we abandon the i_{th} antenna and continue to the above iterative process until only M antennas are left. And the remaining M antennas compose the optimal reconstructed PSA. The

Algorithm 1 Select the optimal M-antenna PSA with CM approach

Require: M, N, $\hat{\mathbf{V}}$, the number of iterations k.
Ensure: $\mathbf{z}$.
  initialize $\mathbf{z} = \mathbf{1}$, $k = 0$.
  for $k = 0$; $k \leq N - K$; $k++$ **do**
    $i = \arg\max_{l=1,\ldots,N} \sum_{j=1}^{N} \hat{\mathbf{V}}_{jl}$;
    $\mathbf{z}(i) = 0$;
    for $g = 1$ to N **do**
      $\hat{\mathbf{V}}_{ig} = 0$;
      $\hat{\mathbf{V}}_{gi} = 0$;
    end for
  end for

detailed procedure of the CM approach is depicted in Algorithm 1.

The entire procedure includes $(N+M-1)(N-M)/2$ additions and $(N-K)(N-1)$ subtractions, enjoying a relatively low computation of order $O\left(N^2\right)$. Therefore, the CM approach is efficient to solve the problem of antenna selection. And its effectiveness will be verified in the following section.

4 Simulation Results

In this section, several simulations under the applications of GNSS are utilized to validate the correctness and effectiveness of the proposed reconfiguration approach. A 4×4-antenna square planar PSA, shown in Fig. 1, is considered, and the antennas are spaced at half wavelength. And we assume that SNR and INR are -20 dB and 60 dB, respectively.

In the first example, we verify the relationship between PSCC and the optimal SINR. A desired signal is coming from $\theta_s = 45°$ and $\phi_s = 30°$. The azimuth of the interference is $\phi_i = 25°$, and the elevation angle changes from $0°$ to $90°$. And the polarization parameters of the interference are $\gamma_i = 0.25\pi$ and $\eta_i = -0.25\pi$. The values of PSCC and SINR under different cases are depicted in Fig. 3. Obviously, the PSCC and SNR show opposite variation tendency, and the SINR increases with PSCC decreasing, verifying the relationship between PSCC and the optimal SINR in (14).

In the second example, the whole process of PSA reconfiguration is illustrated. The DOAs of the desired signal are $\theta_s = 35°$ and $\phi_s = 60°$. The interference comes from $\theta_i = 30°$ and $\phi_i = 72°$, and its polarization parameters are $\gamma_i = 0.4\pi$ and $\eta_i = -0.5\pi$. The target of PSA reconfiguration is achieving the largest SINR with the fewest antennas. The upper bounds of the optimal SINR acquired with three approaches are shown in Fig. 4. And the upper bound gained with the enumeration method is the true maximum. It can be observed that the three curves almost coincide under different numbers of antennas, which demonstrates the

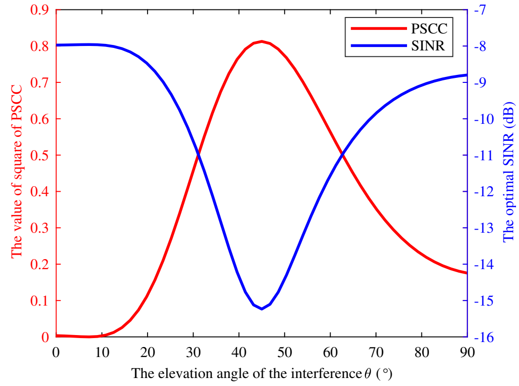

Figure 3. The curves of PSCC and SINR with interference azimuth varying.

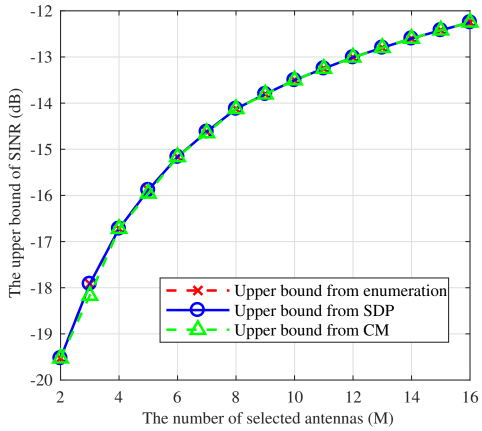

Figure 4. The upper bounds of the optimal SINR acquired with three approaches under different numbers of antennas. The red curve is gotten by enumerating $C_N^M = \frac{N!}{M!(N-M)!}$ possible combinations for each M, the green one and the blue one are severally gained with the SDP and CM method.

effectiveness of the proposed methods in solving the maximum SINR. Besides, compared with the complicated enumeration method, the presented SDP and CM approaches possess lower computational complexity and higher practicability.

According to the result in Fig. 4, we calculate $\mathrm{SINR}_{\mathrm{loss}}$ and O_{cost} with (22) and (23). Then the trade-off curve between computational cost and performance loss is obtained in Fig. 5. Add the constraint that the maximum $\mathrm{SINR}_{\mathrm{loss}}$ cannot be greater than -1.5 dB. we can learn from Fig. 5 that the 10-antenna PSA satisfies the above design requirement while can save the most computational cost. Thus, we choose 10 as the optimal number of antennas, i.e., $M = 10$. Then, utilizing the CM approach, we calculate the optimal reconstructed PSA comprising 10 antennas. And corresponding to the antenna layout in Fig. 1, the PSA after reconfiguration is depicted in Fig. 6. Compared with the primal PSA, the reconstructed PSA saves 75.6% of computation only at the cost of -1.35 dB performance loss. Therefore, we can

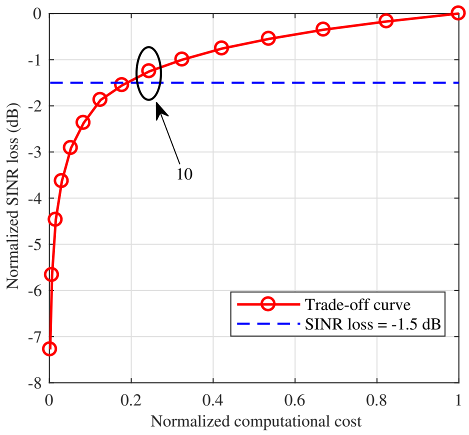

Figure 5. Trade-off curve between computational cost and performance loss.

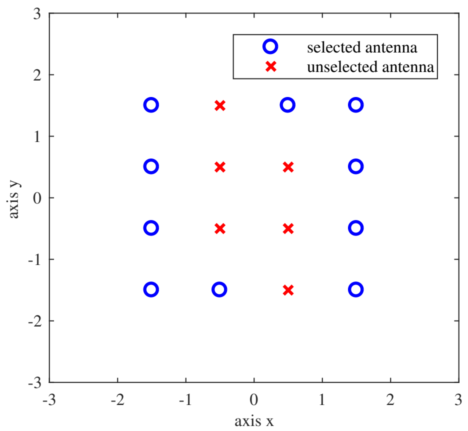

Figure 6. The PSA reconfiguration results of selecting 10 out of 16 antennas. The blue circle and red cross separately indicate that the corresponding antennas are used and abandoned.

conclude that the developed PSA reconfiguration method based on antenna selection is effective in saving cost as well as achieving superior anti-interference performance.

5 Conclusion

In this paper, a PSA reconfiguration method resorting to antenna selection is presented for GNSS interference suppression. Compared with the primal PSA, the reconstructed PSA employs fewer antennas and RF front ends and achieves sufficiently good anti-interference performance. After deriving the optimal SINR based on adaptive processing, we propose the PSCC to describe the influence of PSA reconfiguration on interference suppression performance. Then the SINR maximization problem is transformed into PSCC minimization problem, and we thereby build the mathematical model of antenna selection. To address the nonconvex optimization problem, we present a relaxation approach and successfully solve the upper bound of the optimal SINR. Subsequently, we define two parameters and plot the trade-off curve to guide the selection of the optimal number of antennas. A CM approach is then utilized to substitute the enumeration method to confirm the antennas layout of the reconstructed PSA efficiently. Simulation results demonstrate the effectiveness of the developed reconfiguration approaches.

6 Acknowledgements

This work is supported by National Natural Science Foundation of China under Grant No.61771404, No. 61971355, No. 61901391.

References

[1] M. Xie, W. Xia, S. Wei, H. Li, and P. Li, "A robust GNSS interference suppression method based on null broadening of dual-polarized antenna arrays," in *2018 14th IEEE International Conference on Signal Processing (ICSP)*, 2018, pp. 197–202.

[2] X. Zhenhai, L. Jiajia, S. Longfei, and X. Shunping, "Filtering performance of polarization sensitive array," in *2005 IEEE International Symposium on Microwave, Antenna, Propagation and EMC Technologies for Wireless Communications*, vol. 1, 2005, pp. 212–215 Vol. 1.

[3] R. Compton, "On the performance of a polarization sensitive adaptive array," *IEEE Trans. Antennas Propag.*, vol. 29, no. 5, pp. 718–725, 1981.

[4] J. LaMance, D. Small, and Ion, *Locata Correlator-Based Beam Forming Antenna Technology for Precise Indoor Positioning and Attitude*. Washington: Inst Navigation, 2011, pp. 2436–2445.

[5] P. Rocca, R. L. Haupt, and A. Massa, "Interference suppression in uniform linear arrays through a dynamic thinning strategy," *IEEE Trans. Antennas Propag.*, vol. 59, no. 12, pp. 4525–4533, 2011.

[6] L. Cen, Z. L. Yu, W. Ser, and W. Cen, "Linear aperiodic array synthesis using an improved genetic algorithm," *IEEE Trans. Antennas Propag.*, vol. 60, no. 2, pp. 895–902, 2012.

[7] Y. Liu, Q. H. Liu, and Z. Nie, "Reducing the number of elements in the synthesis of shaped-beam patterns by the forward-backward matrix pencil method," *IEEE Trans. Antennas Propag.*, vol. 58, no. 2, pp. 604–608, 2010.

[8] G. Oliveri, M. Carlin, and A. Massa, "Complex-weight sparse linear array synthesis by bayesian compressive sampling," *IEEE Trans. Antennas Propag.*, vol. 60, no. 5, pp. 2309–2326, 2012.

[9] X. Wang, M. G. Amin, and X. Cao, “Optimum array configurations of maximum output snr for quiescent beamforming,” in *Proc. IEEE Int. Conf. Acoust.,Speech, Signal Process.. (ICASSP), 2017*, 2017, pp. 6274–6278.

[10] X. Wang, M. Amin, and X. Cao, “Analysis and design of optimum sparse array configurations for adaptive beamforming,” *IEEE Trans. Signal Process.*, vol. 66, no. 2, pp. 340–351, 2018.

[11] X. Wang, M. S. Greco, and F. Gini, “Adaptive sparse array beamformer design by regularized complementary antenna switching,” *IEEE Trans. Signal Process.*, vol. 69, pp. 2302–2315, 2021.

[12] S. A. Hamza and M. G. Amin, “Hybrid sparse array beamforming design for general rank signal models,” *IEEE Trans. Signal Process.*, vol. 67, no. 24, pp. 6215–6226, 2019.

[13] H. Nosrati, E. Aboutanios, and D. Smith, “Multistage antenna selection for adaptive beamforming in mimo radar,” *IEEE Trans. Signal Process.*, vol. 68, pp. 1374–1389, 2020.

[14] X. Yu, G. Cui, J. Yang, and L. Kong, “Mimo radar transmit-receive design for moving target detection in signal-dependent clutter,” *IEEE Trans. Veh. Technol.*, vol. 69, no. 1, pp. 522–536, 2020.

[15] L. C. Godara, “Application of antenna arrays to mobile communications. ii. beam-forming and direction-of-arrival considerations,” *Proc IEEE*, vol. 85, no. 8, pp. 1195–1245, 1997.

[16] N. Sidiropoulos, T. Davidson, and Z.-Q. Luo, “Transmit beamforming for physical-layer multicasting,” *IEEE Trans Signal Process.*, vol. 54, no. 6, pp. 2239–2251, 2006.

[17] M. Grant and S. Boyd, “CVX: Matlab software for disciplined convex programming, version 2.1,” http://cvxr.com/cvx, Mar. 2014.

[18] Michael Grant and Stephen Boyd, “Graph implementations for nonsmooth convex programs,” in *Recent Advances in Learning and Control*, ser. Lecture Notes in Control and Information Sciences, V. Blondel, S. Boyd, and H. Kimura, Eds. Springer-Verlag Limited, 2008, pp. 95–110.